

# A Search for Leptoquarks at HERA

H1 Collaboration

## Abstract

A search for leptoquarks at HERA was performed in H1 using 1994  $e^+p$  data corresponding to an integrated luminosity of about  $3 \text{ pb}^{-1}$ . Single leptoquarks were searched for in direct positron-quark fusion processes taking into account possible decays into lepton-quark pairs of either the first, the second, or the third generation. No significant deviation from the Standard Model predictions is found in the various final states studied and mass dependent exclusion limits are derived on the Yukawa couplings of the leptoquarks. Compared with earlier results from an analysis of  $e^-p$  data, exclusion limits are considerably improved for leptoquarks which could be produced via  $e^+$ -*valence quark* fusion. For leptoquarks with lepton flavour conserving couplings, masses up to 275 GeV (depending on the leptoquark type) are excluded for coupling values larger than  $\sqrt{4\pi\alpha_{em}}$ . For leptoquarks with lepton flavour violating couplings, masses up to 225 GeV are excluded for the first time in a direct search for couplings with leptons of the second or third generation larger than  $\sqrt{4\pi\alpha_{em}}$ . Fourteen possible combinations of couplings are studied and stringent exclusion limits comparable or better than any existing direct or indirect limits are obtained for each leptoquark type.

S. Aid<sup>14</sup>, V. Andreev<sup>26</sup>, B. Andrieu<sup>29</sup>, R.-D. Appuhn<sup>12</sup>, M. Arpagaus<sup>37</sup>, A. Babaev<sup>25</sup>,  
 J. Bähr<sup>36</sup>, J. Bán<sup>18</sup>, Y. Ban<sup>28</sup>, P. Baranov<sup>26</sup>, E. Barrelet<sup>30</sup>, R. Barschke<sup>12</sup>, W. Bartel<sup>12</sup>,  
 M. Barth<sup>5</sup>, U. Bassler<sup>30</sup>, H.P. Beck<sup>38</sup>, H.-J. Behrend<sup>12</sup>, A. Belousov<sup>26</sup>, Ch. Berger<sup>1</sup>,  
 G. Bernardi<sup>30</sup>, R. Bernet<sup>37</sup>, G. Bertrand-Coremans<sup>5</sup>, M. Besançon<sup>10</sup>, R. Beyer<sup>12</sup>,  
 P. Biddulph<sup>23</sup>, P. Bispham<sup>23</sup>, J.C. Bizot<sup>28</sup>, V. Blobel<sup>14</sup>, K. Borrás<sup>9</sup>, F. Botterweck<sup>5</sup>,  
 V. Boudry<sup>29</sup>, A. Braemer<sup>15</sup>, W. Braunschweig<sup>1</sup>, V. Brisson<sup>28</sup>, D. Bruncko<sup>18</sup>, C. Brune<sup>16</sup>,  
 R. Buchholz<sup>12</sup>, L. Büngener<sup>14</sup>, J. Bürger<sup>12</sup>, F.W. Büsler<sup>14</sup>, A. Buniatian<sup>12,39</sup>, S. Burke<sup>19</sup>,  
 M.J. Burton<sup>23</sup>, G. Buschhorn<sup>27</sup>, A.J. Campbell<sup>12</sup>, T. Carli<sup>27</sup>, F. Charles<sup>12</sup>, M. Charlet<sup>12</sup>,  
 D. Clarke<sup>6</sup>, A.B. Clegg<sup>19</sup>, B. Clerbaux<sup>5</sup>, S. Cocks<sup>20</sup>, J.G. Contreras<sup>9</sup>, C. Cormack<sup>20</sup>,  
 J.A. Coughlan<sup>6</sup>, A. Courau<sup>28</sup>, M.-C. Cousinou<sup>24</sup>, Ch. Coutures<sup>10</sup>, G. Cozzika<sup>10</sup>,  
 L. Criegee<sup>12</sup>, D.G. Cussans<sup>6</sup>, J. Cvach<sup>31</sup>, S. Dagoret<sup>30</sup>, J.B. Dainton<sup>20</sup>, W.D. Dau<sup>17</sup>,  
 K. Daum<sup>35</sup>, M. David<sup>10</sup>, C.L. Davis<sup>19</sup>, B. Delcourt<sup>28</sup>, L. Del Buono<sup>30</sup>, A. De Roeck<sup>12</sup>,  
 E.A. De Wolf<sup>5</sup>, M. Dirkmann<sup>9</sup>, P. Dixon<sup>19</sup>, P. Di Nezza<sup>33</sup>, W. Dlugosz<sup>8</sup>, C. Dollfus<sup>38</sup>,  
 J.D. Dowell<sup>4</sup>, H.B. Dreis<sup>2</sup>, A. Drouskoi<sup>25</sup>, J. Duboc<sup>30</sup>, D. Düllmann<sup>14</sup>, O. Dünker<sup>14</sup>,  
 H. Duhm<sup>13</sup>, J. Ebert<sup>35</sup>, T.R. Ebert<sup>20</sup>, G. Eckerlin<sup>12</sup>, V. Efremenko<sup>25</sup>, S. Egli<sup>38</sup>,  
 R. Eichler<sup>37</sup>, F. Eisele<sup>15</sup>, E. Eisenhandler<sup>21</sup>, R.J. Ellison<sup>23</sup>, E. Elsen<sup>12</sup>, M. Erdmann<sup>15</sup>,  
 W. Erdmann<sup>37</sup>, E. Evrard<sup>5</sup>, A.B. Fahr<sup>14</sup>, L. Favart<sup>5</sup>, A. Fedotov<sup>25</sup>, D. Feeken<sup>14</sup>,  
 R. Felst<sup>12</sup>, J. Feltesse<sup>10</sup>, J. Ferencei<sup>18</sup>, F. Ferrarotto<sup>33</sup>, K. Flamm<sup>12</sup>, M. Fleischer<sup>9</sup>,  
 M. Flieser<sup>27</sup>, G. Flügge<sup>2</sup>, A. Fomenko<sup>26</sup>, B. Fominykh<sup>25</sup>, M. Forbush<sup>8</sup>, J. Formánek<sup>32</sup>,  
 J.M. Foster<sup>23</sup>, G. Franke<sup>12</sup>, E. Fretwurst<sup>13</sup>, E. Gabathuler<sup>20</sup>, K. Gabathuler<sup>34</sup>,  
 F. Gaede<sup>27</sup>, J. Garvey<sup>4</sup>, J. Gayler<sup>12</sup>, M. Gebauer<sup>9</sup>, A. Gellrich<sup>12</sup>, H. Genzel<sup>1</sup>,  
 R. Gerhards<sup>12</sup>, A. Glazov<sup>36</sup>, U. Goerlach<sup>12</sup>, L. Goerlich<sup>7</sup>, N. Gogitidze<sup>26</sup>, M. Goldberg<sup>30</sup>,  
 D. Goldner<sup>9</sup>, K. Golec-Biernat<sup>7</sup>, B. Gonzalez-Pineiro<sup>30</sup>, I. Gorelov<sup>25</sup>, C. Grab<sup>37</sup>,  
 H. Grässler<sup>2</sup>, R. Grässler<sup>2</sup>, T. Greenshaw<sup>20</sup>, R. Griffiths<sup>21</sup>, G. Grindhammer<sup>27</sup>,  
 A. Gruber<sup>27</sup>, C. Gruber<sup>17</sup>, J. Haack<sup>36</sup>, D. Haidt<sup>12</sup>, L. Hajduk<sup>7</sup>, O. Hamon<sup>30</sup>,  
 M. Hampel<sup>1</sup>, M. Hapke<sup>12</sup>, W.J. Haynes<sup>6</sup>, G. Heinzelmann<sup>14</sup>, R.C.W. Henderson<sup>19</sup>,  
 H. Henschel<sup>36</sup>, I. Herynek<sup>31</sup>, M.F. Hess<sup>27</sup>, W. Hildesheim<sup>12</sup>, K.H. Hiller<sup>36</sup>, C.D. Hilton<sup>23</sup>,  
 J. Hladký<sup>31</sup>, K.C. Hoeger<sup>23</sup>, M. Höppner<sup>9</sup>, D. Hoffmann<sup>12</sup>, T. Holtom<sup>20</sup>,  
 R. Horisberger<sup>34</sup>, V.L. Hudgson<sup>4</sup>, M. Hütte<sup>9</sup>, H. Hufnagel<sup>15</sup>, M. Ibbotson<sup>23</sup>,  
 H. Itterbeck<sup>1</sup>, M.-A. Jabiol<sup>10</sup>, A. Jacholkowska<sup>28</sup>, C. Jacobsson<sup>22</sup>, M. Jaffre<sup>28</sup>,  
 J. Janoth<sup>16</sup>, T. Jansen<sup>12</sup>, L. Jönsson<sup>22</sup>, K. Johannsen<sup>14</sup>, D.P. Johnson<sup>5</sup>, L. Johnson<sup>19</sup>,  
 H. Jung<sup>10</sup>, P.I.P. Kalmus<sup>21</sup>, M. Kander<sup>12</sup>, D. Kant<sup>21</sup>, R. Kaschowicz<sup>2</sup>, U. Kathage<sup>17</sup>,  
 J. Katzy<sup>15</sup>, H.H. Kaufmann<sup>36</sup>, S. Kazarian<sup>12</sup>, I.R. Kenyon<sup>4</sup>, S. Kermiche<sup>24</sup>, C. Keuker<sup>1</sup>,  
 C. Kiesling<sup>27</sup>, M. Klein<sup>36</sup>, C. Kleinwort<sup>12</sup>, G. Knies<sup>12</sup>, W. Ko<sup>8</sup>, T. Köhler<sup>1</sup>, J.H. Köhne<sup>27</sup>,  
 H. Kolanoski<sup>3</sup>, F. Kole<sup>8</sup>, S.D. Kolya<sup>23</sup>, V. Korbel<sup>12</sup>, M. Korn<sup>9</sup>, P. Kostka<sup>36</sup>,  
 S.K. Kotelnikov<sup>26</sup>, T. Krämerkämper<sup>9</sup>, M.W. Krasny<sup>7,30</sup>, H. Krehbiel<sup>12</sup>, D. Krücker<sup>2</sup>,  
 U. Krüger<sup>12</sup>, U. Krüner-Marquis<sup>12</sup>, H. Küster<sup>22</sup>, M. Kuhlen<sup>27</sup>, T. Kurča<sup>36</sup>, J. Kurzhöfer<sup>9</sup>,  
 D. Lacour<sup>30</sup>, B. Laforge<sup>10</sup>, F. Lamarche<sup>29</sup>, R. Lander<sup>8</sup>, M.P.J. Landon<sup>21</sup>, W. Lange<sup>36</sup>,  
 U. Langenegger<sup>37</sup>, P. Lanius<sup>27</sup>, J.-F. Laporte<sup>10</sup>, A. Lebedev<sup>26</sup>, F. Lehner<sup>12</sup>,  
 C. Leverenz<sup>12</sup>, S. Levonian<sup>26</sup>, Ch. Ley<sup>2</sup>, G. Lindström<sup>13</sup>, M. Lindstroem<sup>22</sup>, J. Link<sup>8</sup>,  
 F. Linsel<sup>12</sup>, J. Lipinski<sup>14</sup>, B. List<sup>12</sup>, G. Lobo<sup>28</sup>, P. Loch<sup>28</sup>, H. Lohmander<sup>22</sup>,  
 J.W. Lomas<sup>23</sup>, G.C. Lopez<sup>13</sup>, V. Lubimov<sup>25</sup>, D. Lüke<sup>9,12</sup>, N. Magnussen<sup>35</sup>,  
 E. Malinowski<sup>26</sup>, S. Mani<sup>8</sup>, R. Maraček<sup>18</sup>, P. Marage<sup>5</sup>, J. Marks<sup>24</sup>, R. Marshall<sup>23</sup>,  
 J. Martens<sup>35</sup>, G. Martin<sup>14</sup>, R. Martin<sup>20</sup>, H.-U. Martyn<sup>1</sup>, J. Martyniak<sup>7</sup>, S. Masson<sup>2</sup>,  
 T. Mavroidis<sup>21</sup>, S.J. Maxfield<sup>20</sup>, S.J. McMahon<sup>20</sup>, A. Mehta<sup>6</sup>, K. Meier<sup>16</sup>, T. Merz<sup>36</sup>,

A. Meyer<sup>12</sup>, A. Meyer<sup>14</sup>, H. Meyer<sup>35</sup>, J. Meyer<sup>12</sup>, P.-O. Meyer<sup>2</sup>, A. Migliori<sup>29</sup>,  
S. Mikocki<sup>7</sup>, D. Milstead<sup>20</sup>, J. Moeck<sup>27</sup>, F. Moreau<sup>29</sup>, J.V. Morris<sup>6</sup>, E. Mroczko<sup>7</sup>,  
D. Müller<sup>38</sup>, G. Müller<sup>12</sup>, K. Müller<sup>12</sup>, P. Murín<sup>18</sup>, V. Nagovizin<sup>25</sup>, R. Nahnhauser<sup>36</sup>,  
B. Naroska<sup>14</sup>, Th. Naumann<sup>36</sup>, P.R. Newman<sup>4</sup>, D. Newton<sup>19</sup>, D. Neyret<sup>30</sup>,  
H.K. Nguyen<sup>30</sup>, T.C. Nicholls<sup>4</sup>, F. Niebergall<sup>14</sup>, C. Niebuhr<sup>12</sup>, Ch. Niedzballa<sup>1</sup>,  
H. Niggli<sup>37</sup>, R. Nisius<sup>1</sup>, G. Nowak<sup>7</sup>, G.W. Noyes<sup>6</sup>, M. Nyberg-Werther<sup>22</sup>, M. Oakden<sup>20</sup>,  
H. Oberlack<sup>27</sup>, U. Obrock<sup>9</sup>, J.E. Olsson<sup>12</sup>, D. Ozerov<sup>25</sup>, P. Palmen<sup>2</sup>, E. Panaro<sup>12</sup>,  
A. Panitch<sup>5</sup>, C. Pascaud<sup>28</sup>, G.D. Patel<sup>20</sup>, H. Pawletta<sup>2</sup>, E. Peppel<sup>36</sup>, E. Perez<sup>10</sup>,  
J.P. Phillips<sup>20</sup>, A. Pieuchot<sup>24</sup>, D. Pitzl<sup>37</sup>, G. Pope<sup>8</sup>, S. Prell<sup>12</sup>, R. Prosi<sup>12</sup>, K. Rabbertz<sup>1</sup>,  
G. Rädcl<sup>12</sup>, F. Raupach<sup>1</sup>, P. Reimer<sup>31</sup>, S. Reinshagen<sup>12</sup>, H. Rick<sup>9</sup>, V. Riech<sup>13</sup>,  
J. Riedlberger<sup>37</sup>, F. Riepenhausen<sup>2</sup>, S. Riess<sup>14</sup>, M. Rietz<sup>2</sup>, E. Rizvi<sup>21</sup>, S.M. Robertson<sup>4</sup>,  
P. Robmann<sup>38</sup>, H.E. Roloff<sup>36</sup>, R. Roosen<sup>5</sup>, K. Rosenbauer<sup>1</sup>, A. Rostovtsev<sup>25</sup>, F. Rouse<sup>8</sup>,  
C. Royon<sup>10</sup>, K. Rüter<sup>27</sup>, S. Rusakov<sup>26</sup>, K. Rybicki<sup>7</sup>, N. Sahlmann<sup>2</sup>, D.P.C. Sankey<sup>6</sup>,  
P. Schacht<sup>27</sup>, S. Schiek<sup>14</sup>, S. Schleich<sup>16</sup>, P. Schleper<sup>15</sup>, W. von Schlippe<sup>21</sup>, D. Schmidt<sup>35</sup>,  
G. Schmidt<sup>14</sup>, A. Schöning<sup>12</sup>, V. Schröder<sup>12</sup>, E. Schuhmann<sup>27</sup>, B. Schwab<sup>15</sup>, F. Sefkow<sup>12</sup>,  
M. Seidel<sup>13</sup>, R. Sell<sup>12</sup>, A. Semenov<sup>25</sup>, V. Shekelyan<sup>12</sup>, I. Sheviakov<sup>26</sup>, L.N. Shtarkov<sup>26</sup>,  
G. Siegmon<sup>17</sup>, U. Siewert<sup>17</sup>, Y. Sirois<sup>29</sup>, I.O. Skillicorn<sup>11</sup>, P. Smirnov<sup>26</sup>, J.R. Smith<sup>8</sup>,  
V. Solochenko<sup>25</sup>, Y. Soloviev<sup>26</sup>, A. Specka<sup>29</sup>, J. Spiekermann<sup>9</sup>, S. Spielman<sup>29</sup>,  
H. Spitzer<sup>14</sup>, F. Squinabol<sup>28</sup>, R. Starosta<sup>1</sup>, M. Steenbock<sup>14</sup>, P. Steffen<sup>12</sup>, R. Steinberg<sup>2</sup>,  
H. Steiner<sup>12,40</sup>, B. Stella<sup>33</sup>, J. Stier<sup>12</sup>, J. Stiewe<sup>16</sup>, U. Stöblein<sup>36</sup>, K. Stolze<sup>36</sup>,  
U. Straumann<sup>38</sup>, W. Struczinski<sup>2</sup>, J.P. Sutton<sup>4</sup>, S. Tapprogge<sup>16</sup>, M. Taševský<sup>32</sup>,  
V. Tchernyshov<sup>25</sup>, S. Tchetchnitski<sup>25</sup>, J. Theissen<sup>2</sup>, C. Thiebaux<sup>29</sup>, G. Thompson<sup>21</sup>,  
P. Truöl<sup>38</sup>, J. Turnau<sup>7</sup>, J. Tutas<sup>15</sup>, P. Uelkes<sup>2</sup>, A. Usik<sup>26</sup>, S. Valkár<sup>32</sup>, A. Valkárová<sup>32</sup>,  
C. Vallée<sup>24</sup>, D. Vandenplas<sup>29</sup>, P. Van Esch<sup>5</sup>, P. Van Mechelen<sup>5</sup>, Y. Vazdik<sup>26</sup>,  
P. Verrecchia<sup>10</sup>, G. Villet<sup>10</sup>, K. Wacker<sup>9</sup>, A. Wagener<sup>2</sup>, M. Wagener<sup>34</sup>, A. Walther<sup>9</sup>,  
B. Waugh<sup>23</sup>, G. Weber<sup>14</sup>, M. Weber<sup>12</sup>, D. Wegener<sup>9</sup>, A. Wegner<sup>27</sup>, H.P. Wellisch<sup>27</sup>,  
L.R. West<sup>4</sup>, T. Wilksen<sup>12</sup>, S. Willard<sup>8</sup>, M. Winde<sup>36</sup>, G.-G. Winter<sup>12</sup>, C. Wittek<sup>14</sup>,  
E. Wunsch<sup>12</sup>, T.P. Yiou<sup>30</sup>, J. Žáček<sup>32</sup>, D. Zarbock<sup>13</sup>, Z. Zhang<sup>28</sup>, A. Zhokin<sup>25</sup>,  
M. Zimmer<sup>12</sup>, F. Zomer<sup>28</sup>, J. Zsembery<sup>10</sup>, K. Zuber<sup>16</sup>, and M. zurNedden<sup>38</sup>

<sup>1</sup> *I. Physikalisches Institut der RWTH, Aachen, Germany<sup>f</sup>*

<sup>2</sup> *III. Physikalisches Institut der RWTH, Aachen, Germany<sup>a</sup>*

<sup>3</sup> *Institut für Physik, Humboldt-Universität, Berlin, Germany<sup>a</sup>*

<sup>4</sup> *School of Physics and Space Research, University of Birmingham, Birmingham, UK<sup>b</sup>*

<sup>5</sup> *Inter-University Institute for High Energies ULB-VUB, Brussels; Universitaire Instelling Antwerpen, Wilrijk; Belgium<sup>c</sup>*

<sup>6</sup> *Rutherford Appleton Laboratory, Chilton, Didcot, UK<sup>b</sup>*

<sup>7</sup> *Institute for Nuclear Physics, Cracow, Poland<sup>d</sup>*

<sup>8</sup> *Physics Department and IIRPA, University of California, Davis, California, USA<sup>e</sup>*

<sup>9</sup> *Institut für Physik, Universität Dortmund, Dortmund, Germany<sup>f</sup>*

<sup>10</sup> *CEA, DSM/DAPNIA, CE-Saclay, Gif-sur-Yvette, France*

<sup>11</sup> *Department of Physics and Astronomy, University of Glasgow, Glasgow, UK<sup>b</sup>*

<sup>12</sup> *DESY, Hamburg, Germany<sup>a</sup>*

<sup>13</sup> *I. Institut für Experimentalphysik, Universität Hamburg, Hamburg, Germany<sup>f</sup>*

<sup>14</sup> *II. Institut für Experimentalphysik, Universität Hamburg, Hamburg, Germany<sup>f</sup>*

- <sup>15</sup> *Physikalisches Institut, Universität Heidelberg, Heidelberg, Germany<sup>a</sup>*
- <sup>16</sup> *Institut für Hochenergiephysik, Universität Heidelberg, Heidelberg, Germany<sup>a</sup>*
- <sup>17</sup> *Institut für Reine und Angewandte Kernphysik, Universität Kiel, Kiel, Germany<sup>a</sup>*
- <sup>18</sup> *Institute of Experimental Physics, Slovak Academy of Sciences, Košice, Slovak Republic<sup>f</sup>*
- <sup>19</sup> *School of Physics and Chemistry, University of Lancaster, Lancaster, UK<sup>b</sup>*
- <sup>20</sup> *Department of Physics, University of Liverpool, Liverpool, UK<sup>b</sup>*
- <sup>21</sup> *Queen Mary and Westfield College, London, UK<sup>b</sup>*
- <sup>22</sup> *Physics Department, University of Lund, Lund, Sweden<sup>g</sup>*
- <sup>23</sup> *Physics Department, University of Manchester, Manchester, UK<sup>b</sup>*
- <sup>24</sup> *CPPM, Université d'Aix-Marseille II, IN2P3-CNRS, Marseille, France*
- <sup>25</sup> *Institute for Theoretical and Experimental Physics, Moscow, Russia*
- <sup>26</sup> *Lebedev Physical Institute, Moscow, Russia<sup>f</sup>*
- <sup>27</sup> *Max-Planck-Institut für Physik, München, Germany<sup>f</sup>*
- <sup>28</sup> *LAL, Université de Paris-Sud, IN2P3-CNRS, Orsay, France*
- <sup>29</sup> *LPNHE, Ecole Polytechnique, IN2P3-CNRS, Palaiseau, France*
- <sup>30</sup> *LPNHE, Universités Paris VI and VII, IN2P3-CNRS, Paris, France*
- <sup>31</sup> *Institute of Physics, Czech Academy of Sciences, Praha, Czech Republic<sup>f,h</sup>*
- <sup>32</sup> *Nuclear Center, Charles University, Praha, Czech Republic<sup>f,h</sup>*
- <sup>33</sup> *INFN Roma and Dipartimento di Fisica, Università "La Sapienza", Roma, Italy*
- <sup>34</sup> *Paul Scherrer Institut, Villigen, Switzerland*
- <sup>35</sup> *Fachbereich Physik, Bergische Universität Gesamthochschule Wuppertal, Wuppertal, Germany<sup>f</sup>*
- <sup>36</sup> *DESY, Institut für Hochenergiephysik, Zeuthen, Germany<sup>f</sup>*
- <sup>37</sup> *Institut für Teilchenphysik, ETH, Zürich, Switzerland<sup>i</sup>*
- <sup>38</sup> *Physik-Institut der Universität Zürich, Zürich, Switzerland<sup>i</sup>*
- <sup>39</sup> *Visitor from Yerevan Phys. Inst., Armenia*
- <sup>40</sup> *On leave from LBL, Berkeley, USA*

<sup>a</sup> *Supported by the Bundesministerium für Forschung und Technologie, FRG under contract numbers 6AC17P, 6AC47P, 6DO57I, 6HH17P, 6HH27I, 6HD17I, 6HD27I, 6KI17P, 6MP17I, and 6WT87P*

<sup>b</sup> *Supported by the UK Particle Physics and Astronomy Research Council, and formerly by the UK Science and Engineering Research Council*

<sup>c</sup> *Supported by FNRS-NFWO, IISN-IIKW*

<sup>d</sup> *Supported by the Polish State Committee for Scientific Research, grant Nos. SPUB/P3/202/94 and 2 PO3B 237 08, and Stiftung fuer Deutsch-Polnische Zusammenarbeit, project no.506/92*

<sup>e</sup> *Supported in part by USDOE grant DE F603 91ER40674*

<sup>f</sup> *Supported by the Deutsche Forschungsgemeinschaft*

<sup>g</sup> *Supported by the Swedish Natural Science Research Council*

<sup>h</sup> *Supported by GA ČR, grant no. 202/93/2423, GA AV ČR, grant no. 19095 and GA UK, grant no. 342*

<sup>i</sup> *Supported by the Swiss National Science Foundation*

# 1 Introduction

The  $ep$  collider HERA is particularly suited for the search for leptoquark colour triplet bosons. Such particles appear naturally in various unifying theories beyond the Standard Model (SM) such as Grand Unified Theories and Superstring inspired  $E_6$  models, and in some Compositeness and Technicolour models. They could be produced singly as  $s$ -channel resonances at HERA by the fusion of the 27.5 GeV initial state lepton with a quark of the 820 GeV incoming proton.

In this paper we present a direct search for leptoquark resonances. The analysis combines the H1 1993  $e^-p$  data [1] and 1994  $e^+p$  data which correspond respectively to an integrated luminosity of  $0.43 \text{ pb}^{-1}$  and  $2.83 \text{ pb}^{-1}$ . Earlier direct searches at HERA for leptoquarks coupling to first generation fermions were presented in [1, 2, 3]. The search for leptoquarks coupling also to either second or third generation fermions is presented here for the first time.

## 2 Phenomenology

We consider all possible scalar ( $S_I$ ) and vector ( $V_I$ ) leptoquarks of weak isospin  $I$  with dimensionless couplings  $\lambda_{ij}^{L,R}$  to lepton-quark pairs, where  $i$  and  $j$  indices denote lepton and quark generations respectively and  $L$  or  $R$  is the chirality of the lepton. Following the phenomenological ansatz of ref. [4] which introduces a general effective Lagrangian obeying the symmetries of the SM, there are 10 different leptoquark isospin multiplets, with couplings to left or right handed fermions<sup>1</sup>. The search can be restricted to pure chiral couplings of the leptoquarks given that deviations from lepton universality in helicity suppressed pseudoscalar meson decays have not been observed [6, 7]. This restriction to couplings with either left- ( $\lambda^L$ ) or right-handed ( $\lambda^R$ ) leptons (i.e.  $\lambda^L \cdot \lambda^R \sim 0$ ), affects only two scalar leptoquarks ( $S_0$  and  $S_{1/2}$ ) and two vector leptoquarks ( $V_0$  and  $V_{1/2}$ ).

We otherwise impose a minimal set of simplifying assumptions:

- one of the leptoquark multiplets is produced dominantly;
- states in the leptoquark isospin doublets and triplets are degenerate in mass;
- there exists only one sizeable coupling of the leptoquarks to any given lepton generation.

This last assumption implies that we consider in the  $s$ -channel at HERA only the production via  $\lambda_{1j}$  where  $j = 1, 2$  (implying a production cross-section scaling approximately in  $\lambda_{1j}^2$ ) followed by a decay either via the same coupling or via a coupling  $\lambda_{kl}$  where  $k \neq 1$  and  $l = 1, 2$  or  $3$ . The former case, where we have a unique sizeable coupling to a single lepton and to a single quark generation, corresponds to a “diagonality” requirement in the lepton and quark sector which circumvents the stringent bounds coming from the absence of flavour changing neutral current processes [6, 7]. In the latter case, which admits more than one coupling of comparable strengths, the above assumption guarantees that each

---

<sup>1</sup>A more detailed discussion of the leptoquark classification scheme may be found in a previous publication [2] or in [4, 5].

coupling leads to a distinct observable final state. This is the case for instance for the striking lepton flavour violating sub-processes  $e + q \rightarrow \mu + q'$  or  $\tau + q'$ .

In the  $s$ -channel, a leptoquark is produced at fixed mass  $M = \sqrt{sx}$  where  $\sqrt{s} \sim 300$  GeV is the energy available in the  $ep$  centre-of-mass frame and  $x$  is the incoming quark momentum fraction. The resonance has an intrinsic width  $\Gamma = \lambda^2 M/16\pi$  for scalar and  $\Gamma = \lambda^2 M/24\pi$  for vector leptoquarks. Hence the production cross-section depends on the quark momentum density in the proton and approximately scales with  $\lambda^2$ . When involving first generation leptons, the decay of the leptoquark into a lepton and a jet leads to signatures which are practically indistinguishable event-by-event from SM neutral (NC) and charged current (CC) deep inelastic scattering (DIS). Statistically, the new signal may however be discriminated on the one hand by the presence of a peak in the invariant mass distribution and, on the other hand, by the specific angular distribution of the decay products which depends on the spin of the leptoquark. For a vector leptoquark  $d\sigma/dy \sim (1-y)^2$  where  $y = \frac{1}{2}(1 + \cos\theta^*)$  is the Bjorken scattering variable in DIS and  $\theta^*$  is the decay polar angle in the leptoquark centre of mass (CM) frame. Scalars decay isotropically in their CM frame leading to a constant  $d\sigma/dy$ . These are markedly different from the  $d\sigma/dy \sim y^{-2}$  distribution expected at fixed  $x$  for the dominant  $t$ -channel photon exchange in neutral current DIS events<sup>2</sup>. Hence, first generation leptoquarks are searched for as DIS-like events at high mass and high  $y$ . In contrast, the  $e + q \rightarrow \mu + q'$  or  $\tau + q'$  (followed by a leptonic decay of the  $\tau$ ) processes lead to exotic signatures and are expected to be essentially background free at high  $Q^2$  ( $Q^2 = sxy$ ).

### 3 The H1 detector

A detailed description of the H1 detector can be found elsewhere [8]. Here we describe only the components relevant for the present analysis in which the event final state involves a lepton (positron, muon or neutrino) with high transverse energy  $E_{T,l}$ , balanced more-or-less by a large amount of hadronic  $E_{T,h}$  flow.

The energy flow is measured in a finely segmented liquid argon (LAr) sampling calorimeter [9] covering the polar angle<sup>3</sup> range  $4^\circ \leq \theta \leq 153^\circ$  and all azimuthal angles. It consists of a lead/argon electromagnetic section followed by a stainless-steel/argon hadronic section. Electron energies are measured with a resolution of  $\sigma(E_e)/E_e \simeq 12\%/\sqrt{E_e} \oplus 1\%$  and hadron energies with  $\sigma(E_h)/E_h \simeq 50\%/\sqrt{E_h} \oplus 2\%$  [10] ( $E$  in GeV) after software energy weighting. The absolute energy scales are known to 2% and 5% for electrons and hadrons respectively. The angular resolution on the scattered electron measured from the electromagnetic shower in the calorimeter is  $\lesssim 4$  mrad. A lead/scintillator electromagnetic backward calorimeter extends the coverage at larger angles ( $155^\circ \leq \theta \leq 176^\circ$ ).

Located inside the calorimeters is the tracking system used here to determine the interaction vertex and to measure the track associated to the final state lepton in exotic event topologies. The main components of this system are central drift and proportional

---

<sup>2</sup>At high momentum transfer,  $Z^0$  and  $W$  exchanges become more important and contribute to less pronounced differences between signal and background.

<sup>3</sup>The incoming proton moves by definition in the forward (i.e.  $z > 0$ ) direction with  $\theta = 0^\circ$  polar angle.

chambers ( $25^\circ \leq \theta \leq 155^\circ$ ), a forward track detector ( $7^\circ \leq \theta \leq 25^\circ$ ) and backward proportional chambers ( $155^\circ \leq \theta \leq 175^\circ$ ). The tracking chambers and calorimeters are surrounded by a superconducting solenoid coil providing a uniform field of 1.15 T within the tracking volume. The instrumented iron return yoke surrounding this coil is used here to measure leakage of hadronic showers. The luminosity is determined from the rate of the Bethe-Heitler process  $ep \rightarrow ep\gamma$  measured in a luminosity monitor as described in [8].

## 4 Analysis

### 4.1 DIS-like signatures

For leptoquarks decaying via a coupling to a positron or a neutrino, we are searching for DIS-like signatures.

#### $e + q$ final states

The selection of event candidates for  $e + q$  final states relies essentially on electron finding and energy-momentum conservation cuts. We require:

1. a primary interaction vertex in the range  $|z - \bar{z}| < 35$  cm with  $\bar{z} = 3.4$  cm;
2. an electron with  $E_{T,e} = E_e \sin \theta_e > 7$  GeV and  $10^\circ \leq \theta_e \leq 145^\circ$  (a range covered by the H1 LAr calorimeter). There must be either only one electron candidate or the candidate with highest  $E_{T,e}$  must be at largest polar angle;
3. a total missing transverse momentum  $P_{T,miss} \approx \sqrt{(\sum E_x)^2 + (\sum E_y)^2} \leq 15$  GeV summed over all energy depositions  $i$  in the calorimeters, with  $E_x^i = E^i \sin \theta^i \cos \phi^i$  and  $E_y^i = E^i \sin \theta^i \sin \phi^i$ ;
4. a minimal loss of longitudinal momentum in the direction of the incident electron, i.e.  $43 \leq \sum (E - P_z) \leq 63$  GeV, with  $P_z^i \approx E^i \cos \theta^i$ ;
5. less than 5 GeV in total in the backward calorimeters ( $\theta \gtrsim 152^\circ$ );
6. a Bjorken  $y_e$ , measured from the final state electron, satisfying  $0.05 < y_e < 0.95$ ;
7. when two electron candidates are found, these two candidates must not be balanced in  $E_{T,e}$  and in azimuth, i.e.  $E_{T,e}^1/E_{T,e}^2 > 1.25$  and  $|\Delta\phi_{1,2} - 180^\circ| > 2^\circ$ ;
8. the event must survive a set of halo and cosmic muon filters;
9. the event must be accepted by LAr electron or transverse energy triggers [8] and be properly in time relative to interacting bunch crossings.

The electron identification, which relies on electromagnetic shower estimators and an isolation criteria, was described in [1]. Cut (1) mainly suppresses beam-wall, beam-residual gas and, with (8), background from cosmic rays and halo muons. Cuts (2) and (4) provide a powerful rejection of photoproduction contamination and, with (3),

eliminate DIS charged current events. Cut (4) also suppresses DIS NC-like events with a very hard  $\gamma$  emitted from the initial state electron. Cut (5) further suppresses DIS (or photoproduction) events at small momentum transfer with a misidentified electron in the LAr calorimeter. Cut (6) avoids the high  $y_e$  region where the largest radiative corrections are expected and the low  $y_e$  region where the  $y_e$  and  $x_e$  resolutions deteriorate severely. Cut (7) removes QED Compton events.

In total, 1800 NC-like events satisfy all the above requirements in the mass range  $M_e > 45$  GeV, where  $M_e$  is reconstructed from the final state electron energy and polar angle using

$$M_e = \sqrt{sx_e} = \sqrt{\frac{Q_e^2}{y_e}}, \quad Q_e^2 = \frac{E_{T,e}^2}{1 - y_e}, \quad y_e = 1 - \frac{E_e - P_{z,e}}{2E_e^0}$$

where  $E_e^0$  is the incident electron beam energy.

In order to compare with SM expectations for DIS NC, we make use of the LEPTO Monte Carlo event generator [11], which includes the lowest order electroweak scattering process with QCD corrections to first order in  $\alpha_s$ , complemented by leading-log parton showers and hadronisation [12]. The parton densities in the proton used throughout are taken from the MRSH [13] parametrisation which is close to recent  $F_2$  structure function measurements at HERA (see [14]). All generated events (corresponding to  $\sim 2.5$  times the integrated luminosity for the  $e^+p$  data) were passed through a detailed Monte Carlo simulation of the H1 detector followed by the full analysis chain. We estimate a mean expected NC background of 1680 events with a systematic uncertainty of  $\pm 102$  events. The systematic uncertainty on the expected background comes from the luminosity measurement (1.8%), from the absolute energy calibration (which translates to a 10% effect) and from finite Monte Carlo statistics (1.5%). Taking into account this systematic error and Poisson statistics, this is compatible to less than a standard deviation with the 1800 events observed in our measurement. At largest masses,  $M_e > 150$  GeV, 43 events are observed in excellent agreement with the SM mean of  $37.2 \pm 8.2$  (syst.) expected.

We further investigated possible contamination from direct and resolved photoproduction events of light and heavy quarks. This was studied on the one hand by looking for events with an electron tagged in the H1 luminosity detector when removing cut (5). This detector has an acceptance of  $\sim 15\%$  for photoproduction events with comparable total transverse energy. No such events are found in the data. On the other hand, an upper limit on the contamination was derived from Monte Carlo studies based on the PYTHIA generator [12]. The parton densities in the photon are taken from the GRV-G LO parametrisation [15]. We estimate the contamination to be  $< 0.7\%$  for  $\gamma + p \rightarrow jet + jet$  (direct and resolved photon processes) and  $< 0.6\%$  from heavy flavour pair production by boson-gluon fusion processes.

The comparison of the measured data and DIS NC predictions is shown in the mass spectra of Fig. 1a. The measured mass spectrum is seen before and after having applied a mass dependent  $y_e$  cut which ranges from 0.5 around  $M_e = 45$  GeV to 0.10 around  $M_e = 250$  GeV. This cut is designed [1] via Monte Carlo studies to optimize the signal significance for scalar leptoquark searches, given the expected background. A similar but less severe  $y_e$  cut is optimized separately for vector leptoquark searches.



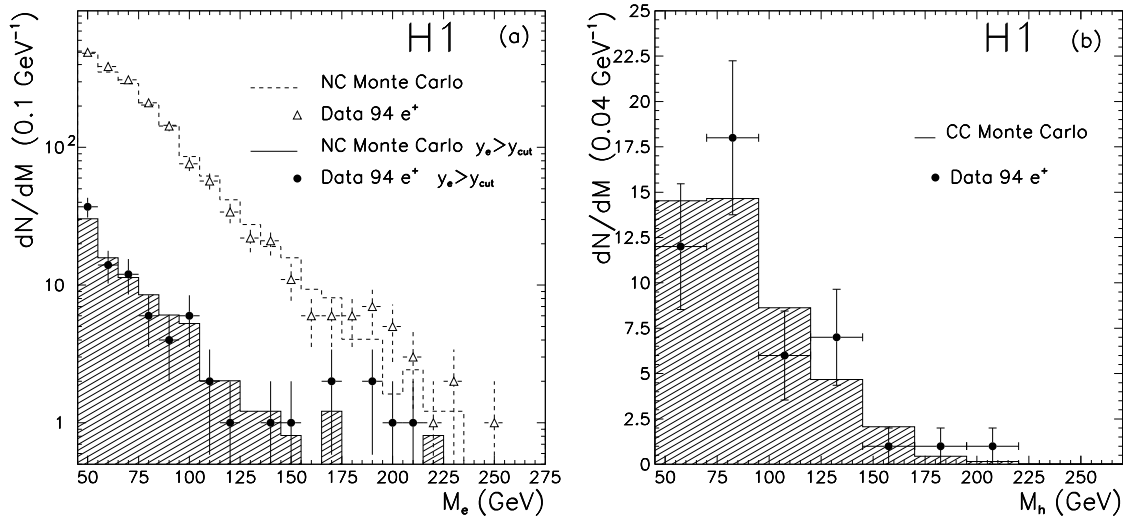


**Figure 1:** Mass spectra for  $e + q$  (a) and  $\nu + q$  (b) final states for data (closed points) and DIS Monte Carlo (shaded histograms). Also shown are the data (open triangles) and DIS NC Monte Carlo (dashed histogram) compared before the final  $y_e$  cut (see text).

In both cases the SM model expectations are in excellent agreement with the data. After the  $y_e$  cut, we observe 91 events while  $84.0 \pm 11.7$  (syst.) events are expected for  $e + q$  data at  $M_e > 45$  GeV. At large masses,  $M_e > 100$  GeV, 13 events are observed in excellent agreement with the mean SM expectation of  $12.4 \pm 3.8$  (syst.). At largest masses,  $M_e > 150$  GeV, 7 events are observed in agreement with the mean expectation of  $3.5 \pm 2.0$  (syst.).

### $\nu + q$ final states

For  $\nu + q$  final states the selection mainly relies on the absence of an electron candidate and large missing momenta. We impose the same primary vertex cuts and apply the same halo and cosmic muon filters as for the  $e + q$  analysis. In addition, we require for the event candidates:

1. no electron satisfying the requirements of the  $e + q$  selection;
2.  $P_{T,miss} > 15$  GeV;
3. a total transverse energy  $E_T \approx \sum |\vec{P}_T|$  roughly matching the total missing transverse momentum  $P_{T,miss}$  such that  $(E_T - P_{T,miss})/E_T < 0.5$ ;
4. at least three charged tracks linked to the primary vertex when the polar angle  $\theta_h$  associated with the hadronic transverse momentum flow ( $\theta_h \approx \tan^{-1} P_{T,miss}/E_T$ ) is within the angular range  $35^\circ \leq \theta_h \leq 155^\circ$ ;

5. the event must be accepted by the LAr missing transverse energy trigger [8] and be properly in time relative to interacting bunch crossings.

Cuts (1), (2) and (3) provide a powerful rejection of photoproduction contamination and eliminate DIS NC events. Halo and cosmic muons which are not accompanied by energy flow in the forward region are rejected by cut (4). We are left at this point with 252 event candidates. We then apply more stringent cosmic and halo filtering algorithms which are cross-checked by visual scan.

In total, 46 CC-like events satisfy all above requirements in the relevant mass range at  $M_h > 45$  GeV where  $M_h$  is reconstructed by summing over all visible final state “hadrons” using

$$M_h = \sqrt{\frac{Q_h^2}{y_h}}, \quad Q_h^2 = \frac{P_{T,miss}^2}{1 - y_h}, \quad y_h = \frac{\sum (E - P_z)}{2E_e^0}.$$

This is in excellent agreement with the SM expectation of  $43.2 \pm 6.8$  (syst.) events obtained using the Monte Carlo DJANGO generator [16] which includes all radiative channels and QCD dipole parton showers. The LAr trigger efficiency losses [17] were folded in. The systematic errors coming from luminosity and energy calibration are similar as for the  $e + q$  channel but here the contribution of the finite Monte Carlo statistic is negligible. The mass spectra for the measured data and DIS CC Monte Carlo predictions shown in Fig. 1b are in excellent agreement over the full mass range.

## 4.2 Exotic signatures

### $\mu + q$ final states

For leptoquarks coupling to a second generation lepton, leading to  $\mu + q$  final states, we can make use of the cuts for the  $\nu + q$  event sample since such events are characterized by a large  $P_{T,miss}$  when calculated from calorimetric quantities. Such  $P_{T,miss}$  is only slightly affected by the minimal energy deposition of the muon. In addition, we require:

1. a charged track linked to the primary vertex within  $\Delta\theta, \Delta\phi < 15^\circ$  around the “muon” angle deduced from the kinematical constraints using the hadronic flow.

The efficiency to find such a charged track was derived from the  $e + q$  event sample by searching on the basis of the hadronic energy flow for the electron track associated with the electron candidate. This efficiency is found to be  $\sim 90\%$  for masses in the range  $45 \leq M_h \leq 225$  GeV. Higher masses lead to a charged lepton falling in an angular domain where no such empirical determination of the efficiency could be made. Cut (1) offers powerful rejection against CC events as it imposes a charged track opposite in azimuth to the current jet. We require no explicit tagging of this “muon” track candidate in the instrumented iron.

We observe no candidate satisfying the  $\mu + q$  selection<sup>4</sup>.

---

<sup>4</sup>It should be noted that the  $e^+p \rightarrow \mu^+X$  event observed by H1 and discussed in [18] fails significantly the kinematical constraints required of a  $eq \rightarrow LQ \rightarrow \mu q'$  event.

## $\tau + q$ final states

For  $\tau + q$  final states, the analysis is restricted to leptonic decays of the  $\tau$  ( $\tau^+ \rightarrow \mu^+ \nu_\mu \bar{\nu}_\tau$  and  $\tau^+ \rightarrow e^+ \nu_e \bar{\nu}_\tau$ ) which constitute  $\sim 36\%$  of all  $\tau$  decays. In the range of large leptoquark masses considered here, the  $\tau$  decay products are generally strongly boosted in the  $\tau$  direction. Hence, the search strategy consists of looking either for  $e + q$  or  $\mu + q$  final states where the  $e$  or the  $\mu$  angle is centered on the  $\tau$  angle deduced from the kinematical constraints using the hadronic energy flow.

For the  $\tau^+ \rightarrow \mu^+ \nu_\mu \bar{\nu}_\tau$  channel, we can make use of the analysis cuts of the above  $\mu + q$  event sample. The  $P_{T,miss}$  measured in the calorimeters is only slightly reduced on average on the quark side when the leptoquark coupling involves a heavy quark which can undergo a semi-leptonic decay. No candidates satisfy these cuts. For the  $\tau^+ \rightarrow e^+ \nu_e \bar{\nu}_\tau$  channel we apply a set of cuts identical to those for the  $\nu + q$  selection except for the following:

1. an electron satisfying the requirements of the  $e + q$  selection, but found within  $\Delta\theta, \Delta\phi < 15^\circ$  around the predicted  $\tau$  angle deduced from the kinematical constraints using the hadronic energy flow;
2.  $P_{T,miss} > 10$  GeV pointing in the azimuthal direction of the  $\tau$ .

Cut (1) imposes a NC-like topology to events otherwise satisfying the  $\nu + q$  selection, hence suppressing DIS CC events. The  $P_{T,miss}$  constraint of cut (2) suppress DIS NC events. We observe no candidate satisfying these cuts for  $M_h \geq 45$  GeV.

## 5 Results

In the absence of any significant deviation from the SM expectations, we now derive rejection limits for Yukawa couplings as a function of mass. For each contributing channel, we use the number of observed events, the signal detection efficiencies and the expected number of background events within a mass bin of variable width (adapted to the expected mass resolution) which slides over the accessible mass range. The statistical procedure which folds in channel per channel the statistical and systematic errors is described in detail in [1]. The signal detection efficiencies are typically determined over a coupling-mass grid with steps in mass of 25 GeV and for coupling values corresponding roughly to the expected ultimate sensitivity to properly take into account the effect on the cross-section of the intrinsic width of the searched resonance. Detailed Monte Carlo simulation of about 500 events per point on the grid is performed followed by the application of the full analysis chain.

For Monte Carlo simulation of leptoquark signals, we make use of the LEGO event generator [19] which was described in more detail in [1]. It takes into account initial state QED radiation and QCD corrections in the initial and final state and corrects properly the kinematics at the decay vertex for effects of the parton shower masses. The efficiencies for the leptoquark signal detection depend only weakly on the leptoquark mass and are given in Table 1 for a typical mass in the middle of the accessible range. For leptoquarks in the  $e + q$  decay channel, the numbers include the effect of the mass dependent  $y_e$  cut

	$S_q$	$S_{\bar{q}}$	$V_q$	$V_{\bar{q}}$
$LQ \rightarrow e + q$	46.2	45.5	48.3	47.3
$LQ \rightarrow \nu + q$		55.5	53.5	
$LQ \rightarrow \mu + q$	73.0	71.7	67.3	56.3
$LQ \rightarrow \tau + q \rightarrow \mu + \nu_\mu + \bar{\nu}_\tau + q$	13.2	13.0	12.2	10.2
$LQ \rightarrow \tau + q \rightarrow e + \nu_e + \bar{\nu}_\tau + q$	10.1	9.9	9.3	7.8

**Table 1:** Leptoquark detection efficiency in % at  $M = 150$  GeV.

and the finite width of the sliding mass bin  $\Delta M_e$  which was optimized and contains about 68% of the signal at a given mass. This  $y_e$  cut for scalars (vectors) varies from  $y_e > 0.5$  (0.25) at 45 GeV to  $y_e > 0.05$  (0.10) at 275 GeV. At 150 GeV, we have  $y_e > 0.35$  (0.20) and  $\Delta M_e \simeq 25$  (40) GeV for scalars (vectors). Comparable efficiencies are obtained for all leptoquarks in this decay channel. The efficiencies are slightly higher for leptoquarks in the  $\nu + q$  decay channel where no mass dependent  $y$  cut is applied. There, at 150 GeV we have  $\Delta M_h \simeq 35$  GeV for all leptoquarks. In the  $\mu + q$  decay channel in which we observed no events and expected no background, the sliding mass bin could be enlarged and contains about 95% of the wanted signal at a given mass while an efficiency loss of 10% comes from the “muon track” identification efficiency. In the  $\tau + q$  channels, the efficiencies include the leptonic branching ratio of the  $\tau$  lepton. They are slightly lower for the  $\tau \rightarrow e + \nu_e + \bar{\nu}_\tau$  case due to the transverse energy requirement for the electron.

Systematic errors entering the exclusion limits derivation, come from the uncertainty on the luminosity measurement and the absolute energy calibration (see section 4.1) and from the choice of the scale entering the structure function calculation (leading to  $\approx 7\%$  uncertainty in the cross-section). The choice of the parton density parametrisation implies an uncertainty of 5% at small mass and 20% at largest mass on the leptoquark cross-sections. The effect of interference between standard DIS processes and leptoquark boson exchange was studied and found to be negligible.

The exclusion limits obtained on the coupling  $\lambda = \lambda_{11}$  at 95% confidence level (CL) are shown in Fig. 2 as a function of the leptoquark mass. The derivation combines the two decay channels (when relevant) with branching ratios determined from the theory [4].

For leptoquarks which in the  $s$ -channel are produced by the fusion of the  $e^+$  with a  $\bar{q}$ , the exclusion domain is only slightly improved compared to our previously published results based only on 1993  $e^-$  beam data [1]. In contrast, considerable improvement is obtained for other leptoquarks which can be produced in  $e^+$ -valence quark fusion. At  $M = 150$  GeV, in the middle of the accessible mass range, the exclusion domain is extended by more than an order of magnitude. This is partly due to the increase of integrated luminosity and partly due to the valence versus sea quark momentum densities in the proton. For these most favourable cases (Fig. 2c and d), leptoquarks with masses up to about 275 GeV are excluded for coupling strengths stronger than the electromagnetic strength (i.e. for  $\lambda_{11} \gtrsim 0.3 \simeq \sqrt{4\pi\alpha_{em}}$ ). Coupling values down to an order of magnitude weaker than  $\sqrt{4\pi\alpha_{em}}$  are excluded for leptoquarks of masses up to 200 GeV.

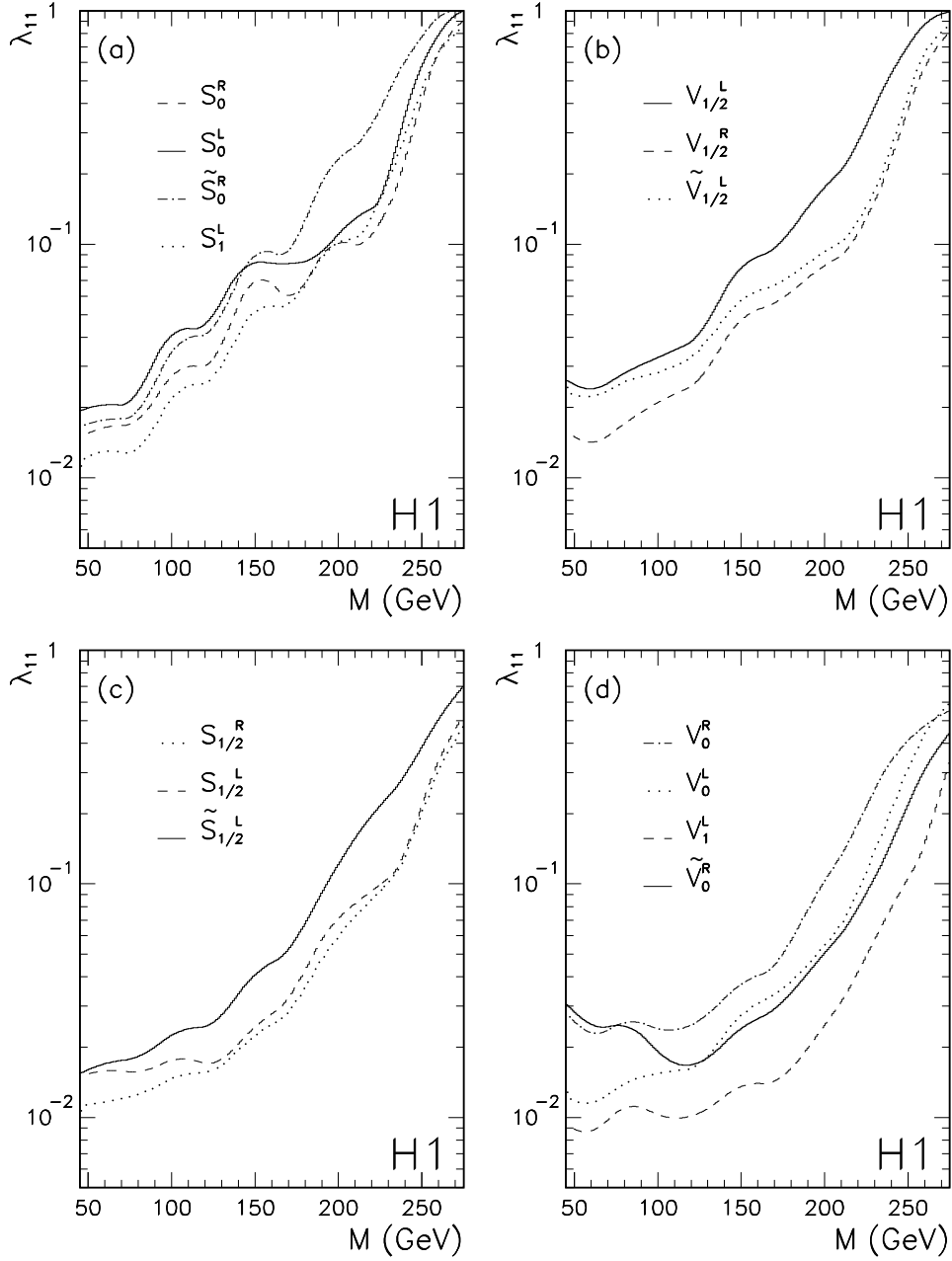


**Figure 2:** Upper limits at 95% CL as a function of mass on the coupling  $\lambda^{L,R}$  for scalar and vector leptoquarks which for an  $e^+$  beam can decay into lepton $+\bar{q}$  (a,b) and lepton $+q$  (c,d). The regions above the curves are excluded. The limits on  $\lambda^L$  for  $S_0, S_1, V_0$  and  $V_1$  combine  $e+q$  and  $\nu+q$  decays. Moreover, limits on  $\lambda^{L,R}$  on (a) and (b) are obtained combining 1993  $e^-p$  and 1994  $e^+p$  data.

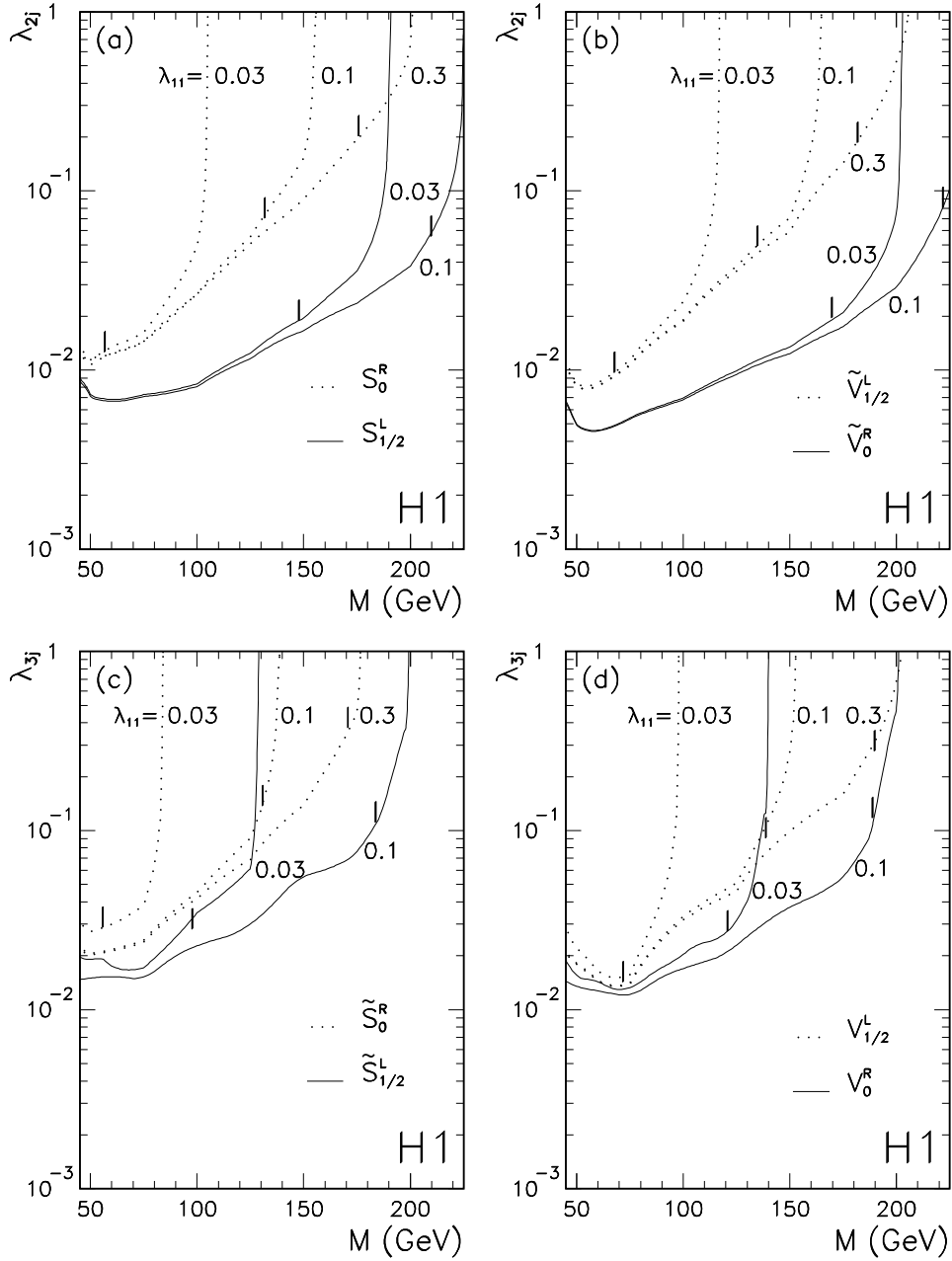


**Figure 3:** Upper limits at 95% CL as a function of mass on the coupling  $\lambda_{2j}$  ( $j = 2, 3$ ) for (a) scalars and (b) vector leptoquarks decaying into  $\mu + q$ , and on the coupling  $\lambda_{3j}$  ( $j = 1, 2, 3$ ) for (c) scalars and (d) vector leptoquarks decaying into  $\tau + q$ . The regions above the curves are excluded. For each leptoquark type, the limits are obtained for different  $\lambda_{11}$  input values. Masses below the symbol | are already excluded by the analysis in the  $e + q$  channel for these given  $\lambda_{11}$ . The limits are obtained using 1994  $e^+p$  data.

The excluded domain in the mass-coupling plane extends beyond the mass range covered by the published results from the D0 experiment at the TEVATRON [20]. The limits obtained there are essentially independent of the Yukawa couplings probed at HERA and in contrast to our results depend significantly on the assumed branching ratios. D0 considers only scalar leptoquarks and rejects masses below 120 (133) GeV at 95% CL for a branching ratio of 0.5 (1.0) into a charged lepton and a quark.

For leptoquarks possessing a coupling  $\lambda_{11}$  to first generation lepton-quark pairs as well as a coupling  $\lambda_{2j}$  ( $\lambda_{3j}$ ) with leptons of the second (third) generation, exclusion limits at 95% CL are shown in Fig. 3 as a function of mass assuming different  $\lambda_{11}$  input values. Here we explicitly make use of the branching fraction into  $\mu + q$  ( $i = 2$ ) or  $\tau + q$  ( $i = 3$ ) final states,  $Br = \lambda_{ij}^2 / (\lambda_{11}^2 + \lambda_{ij}^2)$ . The limits are plotted for representative scalar and vector leptoquarks which couple in the  $s$ -channel to either valence or sea quarks. In the case of a non-vanishing  $\lambda_{11}\lambda_{2j}$  product (Fig. 3a and b), leptoquarks of the chosen types are not excluded from the reach of HERA from indirect searches [6]. The decay of these four leptoquarks ( $S_0^R, S_{1/2}^L, \tilde{V}_{1/2}^L, \tilde{V}_0^R$ ) via  $\lambda_{23}$ , which is forbidden below the top mass, has not been considered here. The leptoquarks chosen for Fig. 3c and d do not couple to the top quark. Masses up to 225 (198) GeV are excluded for the first time in a direct search for couplings with leptons of the second (third) generation larger than  $\sqrt{4\pi\alpha_{em}}$ .

The published results from the CDF experiment at the TEVATRON [21] exclude second generation scalar leptoquarks with masses below 96 (131) GeV at 95% CL with branching ratio 0.5 (1.0) into  $\mu + q$  pairs. However these limits are not directly applicable when more than one coupling is enabled.

Finally, we make use of our knowledge of the expected background, the signal detection efficiencies and the number of observed events in each of the different event topologies considered in section 4 to derive limits on fourteen possible combinations of two couplings. The results are given in Table 2 for a leptoquark mass of  $M = 150$  GeV and equal values of the two couplings. In the case of the diagonal coupling product  $\lambda_{11}\lambda_{11}$ , the limits obtained are comparable or better than any existing direct or indirect limits [6, 7]. In the other case with lepton flavour conserving couplings,  $\lambda_{12}\lambda_{12}$ , stringent limits are established for the first time for most of the leptoquark types. For leptoquarks with lepton flavour violating couplings, exclusion limits better than any existing limits [6] are obtained for each leptoquark type.

## 6 Conclusions

We have searched for leptoquarks with flavour conserving or flavour violating couplings. No evidence for the resonant production of such new particles was found and mass dependent exclusion limits at 95% confidence level were derived for the couplings.

Two flavour conserving cases where only one sizeable coupling exists ( $\lambda_{11}$  or  $\lambda_{12}$ ) were considered. Leptoquarks with masses ranging from 216 GeV to about 275 GeV (depending on the leptoquark flavours) are excluded for  $\lambda_{11}$  coupling values larger than  $\sqrt{4\pi\alpha_{em}}$ . For some of the leptoquark types, the exclusion domain extends down in coupling strength to more than an order of magnitude below our previously published results, and far beyond the mass reach of other existing colliders. Stringent limits on  $\lambda_{12}$  are established for

Leptoquark		$\sqrt{\lambda_{11}\lambda_{11}}$	$\sqrt{\lambda_{11}\lambda_{2j}}$	$\sqrt{\lambda_{11}\lambda_{3j}}$	$\sqrt{\lambda_{12}\lambda_{12}}$	$\sqrt{\lambda_{12}\lambda_{2j}}$	$\sqrt{\lambda_{12}\lambda_{3j}}$
$Q$	Type		$j = 1, 2, 3$	$j = 1, 2, 3$		$j = 1, 2, 3$	$j = 1, 2, 3$
$-1/3$	$S_0^L$	0.084	0.166	0.395	0.162	0.319	0.760 <sub><math>j=2</math></sub>
$-1/3$	$S_0^R$	0.071	0.118 <sub><math>j=2</math></sub> *	0.162 <sub><math>j=2</math></sub> *	0.137	0.227 <sub><math>j=1</math></sub> *	0.312 <sub><math>j=1,2</math></sub> *
$-4/3$	$\tilde{S}_0^R$	0.090	0.107 <sub><math>j=3</math></sub>	0.178 <sub><math>j=2,3</math></sub>	0.123	0.146	0.243 <sub><math>j=1,2,3</math></sub>
$-4/3, -1/3$	$S_1^L$	0.052	0.068 <sub><math>j=3</math></sub>	0.114	0.074	0.098	0.164 <sub><math>j=2,3</math></sub>
$-5/3$	$S_{1/2}^L$	0.025	0.023 <sub><math>j=2</math></sub> *	0.039 <sub><math>j=1,2</math></sub> *	0.244	0.224 <sub><math>j=1</math></sub> *	0.380 <sub><math>j=1,2</math></sub> *
$-5/3, -2/3$	$S_{1/2}^R$	0.023	0.019 <sub><math>j=3</math></sub>	0.036 <sub><math>j=1,2,3</math></sub>	0.140	0.116 <sub><math>j=3</math></sub>	0.219 <sub><math>j=1,2,3</math></sub>
$-2/3$	$\tilde{S}_{1/2}^L$	0.042	0.038 <sub><math>j=3</math></sub>	0.069 <sub><math>j=1,3</math></sub>	0.157	0.142	0.257 <sub><math>j=2,3</math></sub>
$-4/3$	$V_{1/2}^L$	0.082	0.076 <sub><math>j=3</math></sub>	0.133 <sub><math>j=1,3</math></sub>	0.112	0.104 <sub><math>j=2</math></sub>	0.182 <sub><math>j=2,3</math></sub>
$-4/3, -1/3$	$V_{1/2}^R$	0.048	0.059 <sub><math>j=3</math></sub>	0.095 <sub><math>j=1,2,3</math></sub>	0.074	0.091 <sub><math>j=2</math></sub>	0.147 <sub><math>j=1,2,3</math></sub>
$-1/3$	$\tilde{V}_{1/2}^L$	0.059	0.082 <sub><math>j=2</math></sub> *	0.164 <sub><math>j=2</math></sub> *	0.114	0.158 <sub><math>j=1,2</math></sub> *	0.317 <sub><math>j=1,2</math></sub> *
$-2/3$	$V_0^L$	0.028	0.038 <sub><math>j=3</math></sub>	0.072 <sub><math>j=2,3</math></sub>	0.105	0.142 <sub><math>j=2,3</math></sub>	0.269 <sub><math>j=2</math></sub>
$-2/3$	$V_0^R$	0.038	0.029 <sub><math>j=3</math></sub>	0.051 <sub><math>j=1,2,3</math></sub>	0.143	0.109 <sub><math>j=2</math></sub>	0.192 <sub><math>j=1,2,3</math></sub>
$-5/3$	$\tilde{V}_0^R$	0.025	0.017 <sub><math>j=2</math></sub> *	0.031 <sub><math>j=1,2</math></sub> *	0.247	0.168 <sub><math>j=1,2</math></sub> *	0.306 <sub><math>j=1,2</math></sub> *
$-5/3, -2/3$	$V_1^L$	0.014	0.012 <sub><math>j=3</math></sub>	0.020 <sub><math>j=1,3</math></sub>	0.112	0.096 <sub><math>j=2</math></sub>	0.160 <sub><math>j=2,3</math></sub>

**Table 2:** 95% CL upper limits on coupling products at  $M = 150$  GeV. The results on diagonal couplings ( $\sqrt{\lambda_{11}\lambda_{11}}$  and  $\sqrt{\lambda_{12}\lambda_{12}}$ ) are derived combining 1993  $e^-p$  and 1994  $e^+p$  data. Other results rely on 1994  $e^+p$  data and are valid for decays of the leptoquarks involving quarks of the three generations. The results marked with a \* are only valid for the first and second quark generations. The quark generations  $j$  for which our results are better than any existing limits [6] are indicated as subscripts in the table.

the first time for most of the leptoquark types.

Leptoquarks with lepton flavour violating couplings to the first ( $\lambda_{11}$  or  $\lambda_{12}$ ) and second ( $\lambda_{2j}$ ) or third ( $\lambda_{3j}$ ) generation leptons were searched for. Masses up to 225 (198) GeV are excluded for the first time in a direct search for couplings with leptons of the second (third) generation larger than  $\sqrt{4\pi\alpha_{em}}$ . Exclusion limits for combinations of two different couplings better than any other existing limits are obtained.

## Acknowledgements

We are grateful to the HERA machine group whose outstanding efforts made this experiment possible. We appreciate the immense effort of the engineers and technicians who constructed and maintain the detector. We thank the funding agencies for their financial support of the experiment. We wish to thank the DESY directorate for the hospitality extended to the non-DESY members of the collaboration.



## References

- [1] H1 Collaboration, T. Ahmed et al., Z. Phys. C64 (1994) 545.
- [2] H1 Collaboration, I. Abt et al., Nucl. Phys. B396 (1993) 3.
- [3] ZEUS Collaboration, M. Derrick et al., Phys. Lett. B306 (1993) 173.
- [4] W. Buchmüller, R. Rückl and D. Wyler, Phys. Lett. B191 (1987) 442.
- [5] B. Schrempp, Proc. of the Workshop Physics at HERA, DESY, Hamburg (1991), vol. 2 p. 1034, and references therein.
- [6] S. Davidson, D. Bailey and B. Campbell, Z. Phys. C61 (1994) 613.
- [7] M. Leurer, Phys. Rev. D49 (1994) 333; *ibid.* D50 (1994) 536.
- [8] H1 Collaboration, I. Abt et al., DESY preprint 93-103 (July 1993).
- [9] H1 Calorimeter Group, B. Andrieu et al., Nucl. Instr. and. Meth. A336 (1993) 460.
- [10] H1 Calorimeter Group, B. Andrieu et al., Nucl. Instr. and. Meth. A350 (1994) 57; *idem*, Nucl. Instr. and. Meth. A336 (1993) 499.
- [11] LEPTO 6.1; G. Ingelman, Proc. of the Workshop Physics at HERA, DESY, Hamburg (1991), vol. 3 p. 1366.
- [12] PYTHIA 5.6; T. Sjöstrand, Comp. Phys. Comm. 39 (1986) 347; T. Sjöstrand and M. Bengtsson, Comp. Phys. Comm. 43 (1987) 367; JETSET 7.3; T. Sjöstrand, CERN preprint TH-6488-92 (1992).
- [13] A.D. Martin. W.J. Stirling and R.G. Roberts, Phys. Lett B306 (1993) 145; B309 (1993) 492.
- [14] H1 Collaboration, I. Abt et al., Nucl. Phys. B407 (1993) 515, ZEUS Collaboration, M. Derrick et al., Phys. Lett. B316 (1993) 412.
- [15] M. Glück, E. Reya and A.Vogt, Phys. Rev. D45 (1992) 3986; *ibid.* D46 (1992) 1973.
- [16] DJANGO 2.1; G.A. Schuler and H. Spiesberger, Proc. of the Workshop Physics at HERA, DESY, Hamburg (1991), vol. 3 p. 1419.
- [17] H1 Collaboration, S. Aid et al., Z. Phys. C67 (1995) 565.
- [18] H1 Collaboration, T. Ahmed et al., DESY preprint 94-248 (December 1994).
- [19] LEGO 0.02 and SUSSEX 1.5; K. Rosenbauer, dissertation Aachen (in german), PI-THA 95/16, July 1995.
- [20] D0 Collaboration, S. Abachi et al., Phys. Rev. Lett. 72 (1994) 965; see also CDF Collaboration, F. Abe et al., Phys. Rev. D48 (1993) 3939.
- [21] CDF Collaboration, F. Abe et al., Phys. Rev. Lett. 75 (1995) 1012; see also D0 Collaboration, S. Abachi et al., Phys. Rev. Lett. 75 (1995) 3618.